High-density Adherent Culture of CHO Cells Using Rolled Scaffold Bioreactor

Ashkan YekrangSafakar¹, Ali Mehrnezhad¹, Tongyao Wu¹, and Kidong Park^{*1}

¹ Division of Electrical and Computer Engineering, Louisiana State University, Baton Rouge, Louisiana, USA.

*Corresponding author:

Kidong Park, Division of Electrical and Computer Engineering, Louisiana State University, Baton Rouge, 70803, LA, USA.

E-mail: kidongp@lsu.edu - Phone: 225-578-5336

Abstract

Rapid expansion of biopharmaceutical market calls for more efficient and reliable platforms to

culture mammalian cells on a large scale. Stirred-tank bioreactors have been widely used for large-

scale cell culture. However, it requires months of trials and errors to optimize culture conditions

for each cell line. In this paper, we extend our earlier studies on Rolled Scaffold (RS) bioreactors

for high-density adherent cell culture and report two new implementations of RSs with greatly

enhanced mass-manufacturability, termed as Mesh-RS and Fiber-RS. CHO-K1 cells were

successfully expanded in Mesh-RS and Fiber-RS bioreactors with an average growth rate of 1.09

 \pm 0.04 1/day and 0.95 \pm 0.07 1/day, which were higher than those reported in similar studies. Fiber-

RS bioreactor exhibited a very high cell density of 72.8×10⁶ cells/mL. Besides, a dialyzer was

integrated into the RS bioreactor to remove cellular waste and to replenish nutrients without

disturbing the cells. By collecting the dialyzed media separately, the dialysis efficiency was

significantly improved. In conclusion, the developed RS bioreactor has a strong potential to

provide a highly reliable and easily scalable platform for large-scale cell culture in the

biopharmaceutical industry.

Keyword: high-density cell culture, adherent cells, CHO, dialysis culture, bioreactor

1. Introduction

Biopharmaceutical market has seen steady growth in the last few decades (Lu et al., 2020; Walsh, 2018). The industry's market size had increased from \$107 billion in 2010 to over \$188 billion in 2017 (Walsh, 2014, 2018). Therapeutic monoclonal antibodies claim more than half of the sales since 2012 (Grilo & Mantalaris, 2019), and their sales alone are expected to reach \$300 billion by 2025 (Lu et al., 2020). Mammalian cells are currently the most dominant expression platform of therapeutic proteins (Ecker & Seymour, 2020; Whaley & Zeitlin, 2021), and there is a strong need to streamline the large-scale culture of these cells. To this end, the biopharmaceutical industry actively seeks bioreactors that can culture mammalian cells with larger capacity, higher efficiency and reliability, reduced production cost, and shorter commercialization period (Karst, Steinebach, & Morbidelli, 2018; Walker, 2017).

Various cell culture platforms have been developed for large-scale culture of mammalian cells. For adherent culture, there are multilayer flasks (Auniņš et al., 2003; Pakos & Johansson, 1985), packed-bed reactors (Bancroft, Sikavitsas, & Mikos, 2003), hollow fiber bioreactors (Hanley et al., 2014; Mizukami et al., 2018; Roberts et al., 2012; Sheu et al., 2015), and microcarrier culture in stirred-tank bioreactors (Markvicheva & Grandfils, 2004). Multilayer flasks are directly parallelized monolayer culture systems, but they are difficult to scale up (Merten, 2015). Packed-bed reactors and stirred-tank bioreactors with microcarriers suffer from insufficient oxygen transfer, especially with high cell densities (Catapano, Czermak, Eibl, Eibl, & Pörtner, 2009; Martens et al., 1996). In general, bioreactors based on adherent culture provide limited culture capacity and cell density, as it is often found difficult or inefficient for culture media to reach the cells. The multilayer flasks can provide up to 6 m² of capacity (Rowley, Abraham, Campbell, Brandwein, & Oh, 2012), the hollow fiber bioreactors up to 2.1 m² of capacity (Frank,

Jones, Vang, & Coeshott, 2019), and packed-bed bioreactors up to 500 m² of capacity (Valkama et al., 2020).

For suspension culture, there are stirred-tank bioreactors (Reuveny, Velez, Miller, & Macmillan, 1986; Xu & Chen, 2016) and WAVE Bioreactors[™] (M.-F. Clincke et al., 2011; R. Eibl, Werner, & Eibl, 2009). There are also limited cases of hollow fiber bioreactors for suspension culture (De Bartolo et al., 2007; Gardner et al., 2001). Although WAVE bioreactors and hollow fiber bioreactors provide a better microenvironment for the cells than stirred tank bioreactors, they still have inadequate capacities to satisfy industrial demand (D. Eibl & Eibl, 2009).

Currently, suspension culture in stirred-tank bioreactors is the most widely used culture platform in the biopharmaceutical industry for protein production on a large scale (Chu & Robinson, 2001). In these systems, cells are cultured in suspension as single cells or in aggregates while an impeller is continuously stirring the media to suspend the cells and to provide sufficient nutrients and gases uniformly. Stirred-tank bioreactors are difficult to scale up quickly. Larger tank sizes require higher stirring rates to ensure uniform and sufficient transfer of nutrients and gases. However, a higher stirring rate imposes higher shear stress on cells, adversely affecting their growth and production rate (Nienow, 2006; Z. Wang et al., 2020). As such, one would need heuristic approaches to optimize the culture conditions for an extended period of time.

In the biopharmaceutical industry, there is a strong pressure to increase production yield. As the production yield is typically proportional to the number of the recombinant cells and the culture duration, it is advantageous to expand cells quickly and maintain the fully expanded cells as long as possible. A major limiting factor in extending the culture duration of high-density cell cultures is the accumulation of harmful cellular biowastes. For instance, lactate is the most common metabolic byproduct that is routinely monitored during the cell culture process (Tsao et

al., 2005). Its accumulation can acidify the culture medium, which is unfavorable to cells (Lao & Toth, 1997; Ozturk, Riley, & Palsson, 1992). In perfusion culture, the accumulating cellular biowastes are diluted away as the media is continuously exchanged. However, a cell retention mechanism is required to keep the cells inside the bioreactors (Bettinardi, Castan, Medronho, & Castilho, 2020; Woodside, Bowen, & Piret, 1998). Unfortunately, those cell retention devices typically complicate the system (S. Wang et al., 2017) and are susceptible to contaminations (M. F. Clincke et al., 2013). Another approach to removing these byproducts is dialysis, as most cellular biowastes have much smaller molecular weights than target proteins. Dialyzing the media is shown to prolong the culture duration by removing cellular biowastes and replenishing nutrients (Fuchs et al., 2002) while retaining produced target proteins inside the media reservoir. Unfortunately, most dialysis cultures have low efficiency, as they mix the dialyzed medium with the spent one. As a result, the media need to be continuously dialyzed to lower the concentration of cellular biowaste (Fuchs et al., 2002; Märkl, Zenneck, Dubach, & Ogbonna, 1993; Pörtner & Märkl, 1998). Due to these limitations, the dialysis culture is not widely used in the biopharmaceutical industry.

Rolled Scaffold (RS), developed in our earlier study (YekrangSafakar, Hamel, Mehrnezhad, Jung, & Park, 2020), is a platform for high-density adherent culture of mammalian cells. The RS is fabricated by rolling polymer film around a center rod to make spiraled layers in a cylindrical form, as shown in Figure 1a. These layers provide a large surface area for cells to attach to. The gap between layers allows the media to flow through, providing sufficient nutrients and gases to the cells. As shown in Figure 1c, cells are separated from the media reservoir, and the media in the reservoir can be stirred and sparged vigorously and even replaced without harming or losing the cells.

In this study, the RS structure was redesigned for enhanced manufacturability, and a dialysis culture based on the RS bioreactor was demonstrated. In our earlier publication (YekrangSafakar et al., 2020), the first generation of RS, termed as UV-RS in this report, was fabricated through manual UV-imprinting, making it difficult to manufacture large-scale bioreactors. To overcome this issue, we developed Mesh-RS and Fiber-RS, both of which used a feed spacer to control the gap between each layer, as shown in Figure 2a. The feed spacer is commonly used in a reverse osmosis water filter (Haidari, Heijman, & Van Der Meer, 2018). Fiber-RS had an additional layer of non-woven fiber to further increase the surface area for cell attachment. We demonstrated high-density adherent culture with these two types of RSs to prove their functionality. Besides, we implemented a dialysis culture system with the RS bioreactor. The dialyzed media were collected separately rather than mixed with the spent media to greatly enhance dialysis efficiency.

2. Materials and methods

2.1 Fabrication of RS

Mesh-RS was fabricated by rolling a 50 μm-thick polyethylene terephthalate (PET) film (8567K24, McMaster-Carr, USA) and a feed spacer or mesh (Naltex Extruded Netting 115330, Delstar, USA) around a 3.18 mm diameter nylon rod. At the end of the rolling, the rolled film layers were glued with a UV curable adhesive (1187-M, Dymax, USA) and inserted into a RS holder. The UV curable adhesive was cured under a 100W UV LED (light emitting diode) with a peak wavelength at 349 nm for 5 minutes. To fabricate Fiber-RS, the PET film, the feed spacer layer, and a non-woven fiber layer (Reemay 2006, MidWest filtration LLC, USA) were rolled around the same nylon rod. Similarly, the rolled film layers were glued and placed into a RS holder.

To make a RS holder, two syringes were cut, leaving the portion with the luer lock connectors. The RS was inserted into the cut syringes, and the two cut syringes were sealed with the UV curable adhesive, as shown in Figure 2b. 10 mL syringes (309604, BD, USA) were used for small-size RSs, and 30 mL syringes (309650, BD, USA) were used for medium-size RSs.

2.2 Configuration and operation of RS bioreactor

The RS holder was connected to two three-way stopcocks (99781, Qosina, USA) on either side, followed by two oxygen sensors (FTC-SU-PSt3, PreSens, Germany) read by fiber optic oxygen meters (OXY-1 SMA, PreSens, Germany), as shown in Supplementary Figure S1. The two oxygen sensors measured the dissolved oxygen concentration (DO) of the media passing through them. Needleless aseptic connectors (C1000, Clave Connector, ICU medical, Inc., USA) were connected to the third ports of the stopcocks. These were used as access ports to inject the cells into the RS or take samples during the cell expansion. A 100 mL spinner flask (CLS-1430-100, Chemglass, USA) and a 1 L glass bottle (218105403, DURAN, Germany) were used as the media reservoirs for small RS and medium RS, respectively. The media in the reservoirs were stirred by a magnetic stirrer (MS-01UA, Crystal Technology & Industries Inc., USA) at 480 rpm (revolutions per minute). A magnetic stir bar was used in the 1 L reservoir. The RS and the reservoir were connected using 1/16" ID Tygon tubing which passed through a peristaltic pump (Masterflex L/S 77300-40, Cole-Palmer, USA). A multichannel cartridge pump head (Masterflex 7519-20, Cole-Palmer, USA) was used for small-size RS bioreactor with the flow rate in the range of 80 - 5,000 μL/min, and an Easy-Load® II pump head (Masterflex 77200-50, Cole-Palmer, USA) was used for medium-size RS bioreactor with the flow rate in the range of 1,300 - 78,000 μL/min. The media inside the 1 L reservoir was sparged with humidified 5% CO₂ air when the upstream DO decrease to 5.5 mg/L.

2.3 Seeding procedure for RS bioreactors

Prior to seeding cells into the RS, the RS was filled with growth media and incubated for 3 hours. Afterward, the RS was seeded through the upstream access port. Mesh-RS and Fiber-RS were seeded with a cell suspension of 2×10⁵ and 8×10⁵ cells/mL, respectively, to have the target seeding density of 5×10³ cells/cm². The seeded RS was incubated at a 5% CO₂ 37 °C environment without media flow for 3 hours to ensure proper cell attachment.

2.4 Control of media flow rate

The media flow rate was controlled manually with Mesh-RS bioreactors and automatically with Fiber-RS ones. After incubating the seeded RS for 3 hours, the media was circulated at 80 μ L/min for Mesh-RS and 1300 μ L/min for Fiber-RS. As cells grow in number over time, the total oxygen consumption increases, causing the downstream DO to decrease further with increasing cell numbers. In Mesh-RS bioreactors, the flow rate was manually doubled to provide sufficient oxygen to the cells, when downstream DO decreases to 3 mg/L. In Fiber-RS bioreactors, the flow rate was controlled by a computer using a custom MATLAB (MathWorks, USA) script, which increased the flow rate by 10% whenever the downstream DO decreases to 3 mg/L, resulting in significantly more stable downstream DO.

2.5 Characterization of cell growth and culture medium

The DO at upstream and downstream were measured every 2 minutes. The total oxygen consumption rate (OCR_{total}) of the cells inside the RS was calculated as below:

$$OCR_{total} = (DO_{upstream} - DO_{downstream}) \times Q$$

where $DO_{upstream}$ and $DO_{downstream}$ are the DO at upstream and downstream, and Q is the media flow rate. The growth rate, μ , was calculated based on the OCR_{total}:

$$\mu = \frac{\ln(\frac{x_2}{x_1})}{t_2 - t_1}$$

where x_2 and x_1 are the OCR_{total} at times t_2 and t_1 .

The media samples were taken from the upstream access port. Glucose concentration was measured using GlucCellTM (Cesco Bioengineering, Taichung, Taiwan), and lactate concentration was measured by Lactate Plus (J1384N, Nova Biomedical, USA). A standard curve for lactate concentration was generated with lithium lactate (440469, Sigma-Aldrich, USA) solution in the same growth media.

2.6 Harvesting expanded cells in RS bioreactors

After stopping the media flow, PBS (phosphate buffered saline) was injected into the RS through the upstream access port to wash away the culture medium. Then, 0.25% trypsin-EDTA (25200056, Life Technologies, USA) was injected into the RS, and the RS was incubated at 37 °C for 5 minutes. After detaching the cells, the RS was injected with culture media at a high flow rate to collect the detached cells. This process was repeated two more times for higher harvesting efficiency.

2.7 Dialysis setup

The dialysis setup consisted of a dialyzer (114745L-Revaclear 300 dialyzer, Gambro Dialysatoren GmbH, Germany) with a 1.4 m² membrane area, two media reservoirs, two dialysate reservoirs, and a RS bioreactor, as shown in Figure 5a and Supplementary Figure S2. Both ends of the RS were connected to both media reservoirs with three-way stopcock valves to select one reservoir at a time. The two media reservoirs were also connected through the dialyzer.

Initially, the culture media was stored in the first media reservoir and pumped into the RS. During the dialysis, which took about 20 minutes, the media in the first reservoir flowed through the dialyzer at 46 mL/min, while the dialysate (Ham's F-12K, 21127022, Life Technologies, USA) was pumped into the dialysate port in a countercurrent flow at 96 mL/min. Cellular biowastes with low molecular weights in the culture media were moved to the dialysate through the dialyzer's membrane, while target proteins and antibodies with high molecular weight were retained in the culture media. The dialyzed media was collected in the second reservoir to separate them from the undialyzed media in the first reservoir. Once most of the media in the first reservoir was dialyzed, the dialyzed media in the second reservoir was pumped into the RS.

2.8 Cell culture and culture medium

CHO-K1 cells were maintained in T-flasks in a humidified 5% CO₂ environment at 37 °C. The growth media consisted of Ham's F-12K (Kaighn's) Medium (21127022, Life Technologies, USA) supplemented with 10% (v/v) fetal bovine serum (FBS, 10437028, Life Technologies, USA) and 1% (v/v) penicillin streptomycin (15140122, Life Technologies, USA). Cells were subcultured every four days when they reached 70-80% confluency. The same medium was used in the RS bioreactors. 27 mL of concentrated supplement (CHO CD EfficientFeedTM A, Life Technologies, USA) was added to the Fiber-RS reservoirs when glucose levels decreased to 0.25 g/L or below.

3. Results

3.1 Cell expansion in Mesh-RS

We expanded CHO-K1 cells in the Mesh-RS bioreactor and observed the OCR_{total}, which is proportional to the total cell number. The cellular metabolism and the growth were monitored in real-time by measuring the DO of media at upstream and downstream, as shown in Figure 3a. The DO at upstream slowly decreases by about 17% over 4 days, showing that the gas transfer

efficiency in the reservoir was sufficient for the maximum cell population. The downstream sensor shows a lower DO value than the upstream one, as the cells in the RS consume dissolved oxygen in the passing media. As cells proliferate over time, the total oxygen consumption increases and the downstream DO decreases. Each time the downstream DO decrease to 3 mg/L, the flow rate was increased to provide sufficient oxygen to the cells.

The OCR_{total} increased exponentially with an average doubling time of 15.4 ± 0.9 hours, as shown in Figure 3b. To evaluate the growth of CHO-K1 cells in Mesh-RS, three expansions in small-size, denoted by 'Mesh-SRS', and two expansions in medium-size, denoted by 'Mesh-MRS', were performed. Cells in Mesh-SRS were harvested 90 hours after the cell seeding, and the resulting doubling times of 'Mesh-SRS#1', 'Mesh-SRS#2', and 'Mesh-SRS#3' were 14.4, 16.7, 15.7 hours, respectively. Cells in medium-size Mesh-RSs exhibited a similar growth rate to those in the small-size ones. In Mesh-MRS#1, 950 million cells were harvested after 116 hours, indicating a 103-fold increase in the cell population. Cells in Mesh-MRS#2 showed a 66-fold increase in the OCR_{total} over a 99-hour culture period (cells were not harvested from the RS in this experiment). Cells doubling time during Mesh-MRS#1 and Mesh-MRS#2 runs were 14.8 and 15.3 hours, respectively.

OCR_{total} is linearly proportional to the number of cells inside the RS, as shown in Figure 3c. We compared harvested cell counts to the final OCR_{total} value just before harvesting cells to identify the correlation between CHO-K1 cell count and oxygen consumption in the RS bioreactor. The data presented in Figure 3c was collected from multiple cell expansions in UV-RS bioreactors in our previous study (YekrangSafakar et al., 2020) and Mesh-RS bioreactors in this paper. The average cell-specific oxygen uptake rate (OUR_{CHO-K1}) was 39.2 ± 3.5 amol/cell/s, which is similar to the reported values of 55 amol/cell/s (Gray, Chen, Howarth, Inlow, & Maiorella, 1996) and 47-

66.8 amol/cell/s (Goudar, Piret, & Konstantinov, 2011). The RS bioreactor's unique configuration allows for direct and real-time measurement of the OCR_{total}, from which the total cell count and the cellular metabolic level can be extracted based on cell-specific oxygen uptake rate.

To assess the cell proliferation rate with different scales of RS bioreactors, we compared the growth rate and the OUR_{CHO-K1} for small-size and medium-size Mesh-RSs, as shown in Figure 3d and 3e. The average growth rate of cells in Mesh-SRS and Mesh-MRS were 1.09 ± 0.05 1/day and 1.11 ± 0.03 1/day, respectively. Moreover, the OUR_{CHO-K1} were 41.0 amol/cell/s for Mesh-SRS and 42.4 amol/cell/s for Mesh-MRS. Hence, cells' metabolism was consistent regardless of the RS bioreactor size.

3.2 Cell expansion and low-temperature culture in Fiber-RS

Two cell expansions with Fiber-RS bioreactor were performed, labeled as Fiber-RS#1 and Fiber-RS#2 in Figure 4a. Both runs exhibited an exponential growth phase in the first 5 days. Cells in Fiber-RS#1 showed a 103-fold increase in 111 hours based on the OCR_{total}, while cells in Fiber-RS#2 had a 77.5-fold increase in 107 hours. The cell doubling times for these two expansions were 16.6 and 17.0 hours, respectively. Although the cell growth rates in the two expansions were very similar, the fold-increases exhibited some variation due to the difficulties in assessing initial OCR_{total} accurately. On day 6, the OCR_{total} of Fiber-RS#1 showed a gradual saturation, where the total cell number and cell density were estimated at 1670 million and 64.7×10⁶ cell/mL. We believe that this saturation is due to the lack of available surface area for newly divided cells, as the internal surface of the RS is occupied by other cells. The media in the reservoir was exchanged on day 6 to replenish the nutrients at the end of the exponential growth phase. On day 7, the incubator's temperature was lowered to 34 °C to slow down cell proliferation. It is a common practice in the biopharmaceutical industry to reduce the temperature during the protein production phase to slow

the cell metabolism for enhanced protein production (Ahn, Jeon, Jeong, Lee, & Yoon, 2008; Chen, Wu, Liu, Liu, & Huang, 2004; Chuppa et al., 1997; Rodriguez et al., 2010). Cells in Fiber-RS#1 were maintained for 10 days with an occasional supply of the nutrient supplement.

The cumulative consumption of glucose increased exponentially during the growth phase, as shown in Figure 4b. In the Fiber-RS#1 run, the total glucose consumed by cells started to increase linearly after day 6 as the OCR_{total} approached saturation, suggesting a constant glucose consumption. The specific glucose consumption rate (q_{glc}) was analyzed at different cell densities, shown in Figure 4c. For both Fiber-RS runs, q_{glc} reached a steady state of 3.5 pmol/cell/day when cell density increased to 30×10^6 cells/mL. Other high-density culture studies that used CHO cells reported a q_{glc} of 2 pmol/cell/day (M. F. Clincke et al., 2013) and 1.5 pmol/cell/day (Xu & Chen, 2016). Higher q_{glc} in the RS bioreactor suggests that cells in the RS have a higher metabolic rate.

3.3 Dialysis culture in Fiber-RS

We expanded 2 billion cells in the Fiber-RS bioreactor and used a dialyzer in the RS setup to maintain the culture for 10 days without replacing the media, as shown in Figure 5. Using the dialysis module in Figure 5a, we removed cellular biowastes and replenished nutrients at the end of the exponential growth phase on day 5. In the first 125 hours of cell expansion, cells exhibit similar exponential growth to Fiber-RS#1 and Fiber-RS#2, with a doubling time of 18.7 hours. At the end of the growth phase on day 5, the reservoir's media was dialyzed. The dialysis took about 20 minutes, after which the lactate concentration in the media reservoir was reduced by 92%, and the glucose concentration was recovered from 21% to 100% of a fresh media, as shown in Figure 5c. The total amount of glucose and lactate in the main media and the used dialysate remained consistent before and after the dialysis process, as shown in Figure 5d. On day 6, the OCR_{total} reached saturation with the number of cells estimated to be 2 billion, indicating a cell density of

72.8×10⁶ cells/mL. After day 6, the nutrient supplement was periodically added to the reservoir and a high cell density was maintained until day 10.

4. Discussion

4.1 RS bioreactor for large-scale cell culture

The unique design of RS bioreactor has the potential to overcome the existing limitations of current large-scale bioreactors. First, the microenvironment does not vary with increasing RS capacities. As shown in Figure 3, RSs with different capacities have almost the same cell growth characteristics. The capacity of RS is increased by increasing the number of layers with the same composition and gap height, and this ensures an identical microenvironment for cells over different scales. On the contrary, the microenvironments of stirred-tank bioreactors change with their capacities, requiring careful optimization for scaling up. Second, in the RS bioreactor, the medium flows through the gap from upstream to downstream in a laminar flow due to the small gap height. As such, the fluid flow in the RS bioreactor creates much less shear stress on cells and transport nutrients and gases more efficiently. Third, combined metabolic activities of cells or total cell population can be directly monitored in real-time with the upstream and downstream sensors. A real-time assessment of cellular metabolic activities would facilitate the optimization of the culture medium and other operating parameters of the RS bioreactor. Lastly, the culture media is mostly separated from the cells, and the culture media can be aerated, stirred, replaced, or dialyzed without damaging cells, increasing efficiency and flexibility in the bioreactor operation.

On the other hand, the RS bioreactors require cell detachment and seeding, when one wants to further expand the cells in a larger RS-bioreactor. Typically, the cells would need about half a day to fully recover their growth rate, which would slow down the cell expansion to the desired scale. This can be minimized by reducing the initial seeding density and increasing the fold-

increase per each expansion stage. In our recent tests, CHO cells were expanded in T-flasks at 20% of typical seeding concentrations without showing a reduction in the growth rate, suggesting that further optimization of seeding density in RS bioreactors is feasible. Also, current cell lines and media are mostly developed for suspension culture. For the highest production efficiency with the RS bioreactor, cell lines and culture media specifically optimized for adherent culture would be essential. Lastly, with a much larger RS, the preferential flow pathway may form and the media flow may not be evenly distributed. We believe that this can be prevented by using a shower-head setup inside the RS holder, as shown in Supplementary Figure S3.

4.2 Comparison between Mesh-RS, Fiber-RS, and UV-RS

Fiber-RS provides a higher cell culture density compared to Mesh-RS and UV-RS due to the embedded fiber layer. A medium UV-RS with 5.5 mL of internal volume can maintain 960 million cells at its peak confluency and the cell density inside the UV-RS bioreactor is up to 61.8×10⁶ cells/mL. A Mesh-RS with a similar surface area would have 47 mL of internal volume as the gap between its layers is 4.6 times larger than that of UV-RS. The cell density in a Mesh-RS can reach up to 20.4×10⁶ cells/mL. However, Fiber-RS provides up to 72.8×10⁶ cells/mL due to its additional fiber layer that increases the surface area dramatically. The use of feed spacer simplifies the fabrication process of Fiber-RS and Mesh-RS for large-scale production, but we believe that it will result in higher shear stress than UV-RS. Supplementary Table S1 summarizes the key characteristics of each type of RS. In summary, although UV-RS provides great performances, it is very challenging to mass-produce UV-RS without building a complicated roll-to-roll UV imprinting setup. Fiber-RS can be a practical alternative to UV-RS with comparable performances, as Fiber-RS has large-capacity and mass-producibility.

4.3 Cellular growth rate within a RS bioreactor

We compared the growth rate of CHO-K1 cells in the RS to three different perfusion cultures in the literature that achieved cell densities over 50×10⁶ cells/mL, as shown in Figure 6. In this comparison, the cell density of the RS bioreactor is based on the cell population over the RS internal volume rather than the reservoir volume, as similarly done in Zhang et al. (2015). CHO-K1 cells in culture flasks exhibited an average growth rate of 1.078 ± 0.014 1/day or a doubling time of 15.5 hours over six passages. The same cells in RS bioreactors exhibited a comparable growth rate with an average of 0.95 ± 0.07 1/day or a doubling time of 17.5 hours. We maintained the 2 billion cells in RS bioreactor for 11 days and used 2L of media. This is equivalent to cell-specific perfusion rate (CSPR) of 100 pL/cell/day. The growth rate was consistent over different cell densities until the available surface area was depleted and the cell population saturated. Clincke et al. (2013) utilized a disposable WAVE BioreactorTM with an alternating tangential flow (ATF) system for its cell retention to reach the maximum cell density of 101×10⁶ cells/mL with a CSPR of 50-60 pL/cell/day. The growth rate started at 0.7 1/day, but it dropped to 0.35 1/day when the cell density increased above 30×10⁶ cells/mL on day 5. In another study (Zhang et al., 2015), CHO cells were immobilized in a CellTankTM bioreactor. The perfusion culture reached a cell density of 110×10⁶ cells/mL after 13 days with an average growth rate of 0.37 ± 0.1 1/day and a CSPR of 50 pL/cell/day. Finally, Xu & Chen (2016) achieved a cell density of 68.3×10^6 cells/mL in a stirred tank bioreactor with an ATF system. The cells had a steady, nonincreasing growth rate of 0.52 ± 0.09 1/day during the growth phase, with CSPR reported at 23 pL/cell/day. A consistently high growth rate significantly shortens the cell expansion phase in biopharmaceutical production and reduces the time and cost of the upstream process (Bielser, Wolf, Souquet, Broly, & Morbidelli, 2018).

4.4 Using dialysis in the RS bioreactor setup

Dialysis offers an effective method to remove cellular biowastes while retaining macromolecular products in the bioreactor. Other studies (Comer et al., 1990; Frahm, Lane, Märkl, & Pörtner, 2003; Kurosawa, Märkl, Niebuhr-Redder, & Matsumura, 1991) have used dialysis setup before but they suffer from poor efficiency. In these studies, the dialyzed media was not collected separately. The dialyzed media was mixed with the un-dialyzed media and the concentration of cellular biowaste decreased very slowly. Therefore, reducing the lactate level below 50% usually takes several hours (Czermak, Pörtner, & Brix, 2009; Nakano, Rischke, Sato, & Märkl, 1997), even if the dialysis systems has a high membrane area (Fuchs et al., 2002)

The dialysis setup implemented in the RS bioreactor collects the dialyzed media in a separate reservoir, making it highly efficient compared to dialysis systems reported in earlier studies. As the dialyzed media is separated from the spent media, the cellular biowaste can be removed with high efficiency and in a significantly shorter time. In our study, the lactate concentration decreased to 8% in only 20 minutes of dialysis.

5. Conclusion

To keep up with the increasing demands in the biopharmaceutical industry for large-scale production of therapeutic proteins, a reliable and scalable bioreactor is urgently required. In this work, we presented two novel designs of the RS bioreactors. The fabrication processes of these new RSs, Mesh-RS and Fiber-RS, are significantly streamlined and can be automated using a simple roll-to-roll setup. We demonstrated that the Fiber-RS bioreactor could reach a peak cell density of 72.8×10⁶ cells/mL. The fast growth rate of CHO-K1 cells in the RS bioreactors was maintained over a longer period than other comparable high cell density bioreactors. Moreover, we showed the integration of a dialyzer into the RS bioreactor to efficiently remove cellular

biowaste without disturbing cells, to prolong the cell culture without replacing costly media. This has a strong potential to increase yield and reduce media costs significantly. In conclusion, although there are some remaining technical challenges, the RS bioreactor is a highly efficient, reliable, and affordable platform for expanding mammalian cells and has the potential to produce biopharmaceutics with higher productivity on an industrial scale. Besides, the RS bioreactors can be used in other large-scale cell culture applications, where adherent culture is preferred over suspension culture.

Acknowledgments

This material is based upon work supported by the National Science Foundation under Grant No. 1848251.

Conflicts of interest

Louisiana State University owns patents on RS and RS bioreactors.

Data availability statement

The data that support the findings of this study are available from the corresponding author upon reasonable request.

References:

- Ahn, W. S., Jeon, J. J., Jeong, Y. R., Lee, S. J., & Yoon, S. K. (2008). Effect of culture temperature on erythropoietin production and glycosylation in a perfusion culture of recombinant CHO cells. *Biotechnology and bioengineering*, 101(6), 1234-1244.
- Auniņš, J. G., Bader, B., Caola, A., Griffiths, J., Katz, M., Licari, P., . . . Zhou, W. (2003). Fluid mechanics, cell distribution, and environment in cell cube bioreactors. *Biotechnology progress*, 19(1), 2-8.
- Bancroft, G. N., Sikavitsas, V. I., & Mikos, A. G. (2003). Design of a flow perfusion bioreactor system for bone tissue-engineering applications. *Tissue engineering*, *9*(3), 549-554.

- Bettinardi, I. W., Castan, A., Medronho, R. A., & Castilho, L. R. (2020). Hydrocyclones as cell retention device for CHO perfusion processes in single-use bioreactors. *Biotechnology and Bioengineering*.
- Bielser, J.-M., Wolf, M., Souquet, J., Broly, H., & Morbidelli, M. (2018). Perfusion mammalian cell culture for recombinant protein manufacturing—A critical review. *Biotechnology advances*, *36*(4), 1328-1340.
- Catapano, G., Czermak, P., Eibl, R., Eibl, D., & Pörtner, R. (2009). Bioreactor design and scale-up. In *Cell and Tissue Reaction Engineering* (pp. 173-259): Springer.
- Chen, Z.-L., Wu, B.-C., Liu, H., Liu, X.-M., & Huang, P.-T. (2004). Temperature shift as a process optimization step for the production of pro-urokinase by a recombinant Chinese hamster ovary cell line in high-density perfusion culture. *Journal of bioscience and bioengineering*, *97*(4), 239-243.
- Chu, L., & Robinson, D. K. (2001). Industrial choices for protein production by large-scale cell culture. *Current opinion in biotechnology, 12*(2), 180-187.
- Chuppa, S., Tsai, Y. S., Yoon, S., Shackleford, S., Rozales, C., Bhat, R., . . . Naveh, D. (1997). Fermentor temperature as a tool for control of high-density perfusion cultures of mammalian cells. *Biotechnology and bioengineering*, 55(2), 328-338.
- Clincke, M.-F., Mölleryd, C., Zhang, Y., Lindskog, E., Walsh, K., & Chotteau, V. (2011). Study of a recombinant CHO cell line producing a monoclonal antibody by ATF or TFF external filter perfusion in a WAVE Bioreactor™. Paper presented at the BMC proceedings.
- Clincke, M. F., Mölleryd, C., Zhang, Y., Lindskog, E., Walsh, K., & Chotteau, V. (2013). Very high density of CHO cells in perfusion by ATF or TFF in WAVE bioreactor™. Part I. Effect of the cell density on the process. *Biotechnology progress*, 29(3), 754-767.
- Comer, M. J., Kearns, M. J., Wahl, J., Munster, M., Lorenz, T., Szperalski, B., . . . Brunner, H. (1990). Industrial production of monoclonal antibodies and therapeutic proteins by dialysis fermentation. *Cytotechnology*, *3*(3), 295-299.
- Czermak, P., Pörtner, R., & Brix, A. (2009). Special engineering aspects. In *Cell and tissue reaction engineering* (pp. 83-172): Springer.
- De Bartolo, L., Piscioneri, A., Cotroneo, G., Salerno, S., Tasselli, F., Campana, C., . . . Bossio, M. (2007). Human lymphocyte PEEK-WC hollow fiber membrane bioreactor. *Journal of biotechnology*, 132(1), 65-74.
- Ecker, D. M., & Seymour, P. (2020). Supply and demand trends: mammalian biomanufacturing industry overview. *Pharma's year of accelerated innovation & convergence*.
- Eibl, D., & Eibl, R. (2009). Bioreactors for mammalian cells: general overview. *Cell and tissue reaction engineering*, 55-82.
- Eibl, R., Werner, S., & Eibl, D. (2009). Bag bioreactor based on wave-induced motion: characteristics and applications. In *Disposable bioreactors* (pp. 55-87): Springer.
- Frahm, B., Lane, P., Märkl, H., & Pörtner, R. (2003). Improvement of a mammalian cell culture process by adaptive, model-based dialysis fed-batch cultivation and suppression of apoptosis. *Bioprocess and Biosystems Engineering*, 26(1), 1-10.
- Frank, N. D., Jones, M. E., Vang, B., & Coeshott, C. (2019). Evaluation of reagents used to coat the hollow-fiber bioreactor membrane of the Quantum® Cell Expansion System for the culture of human mesenchymal stem cells. *Materials Science and Engineering: C, 96, 77-85*.
- Fuchs, C., Köster, D., Wiebusch, S., Mahr, K., Eisbrenner, G., & Märkl, H. (2002). Scale-up of dialysis fermentation for high cell density cultivation of Escherichia coli. *Journal of biotechnology*, *93*(3), 243-251.
- Gardner, T., Ko, S.-C., Yang, L., Cadwell, J., Chung, L., & Kao, C. (2001). Serum-free recombinant production of adenovirus using a hollow fiber capillary system. *Biotechniques*, *30*(2), 422-427.

- Goudar, C. T., Piret, J. M., & Konstantinov, K. B. (2011). Estimating cell specific oxygen uptake and carbon dioxide production rates for mammalian cells in perfusion culture. *Biotechnology progress*, 27(5), 1347-1357.
- Gray, D. R., Chen, S., Howarth, W., Inlow, D., & Maiorella, B. L. (1996). CO 2 in large-scale and high-density CHO cell perfusion culture. *Cytotechnology*, *22*(1-3), 65-78.
- Grilo, A. L., & Mantalaris, A. (2019). The increasingly human and profitable monoclonal antibody market. *Trends in biotechnology, 37*(1), 9-16.
- Haidari, A., Heijman, S., & Van Der Meer, W. (2018). Optimal design of spacers in reverse osmosis. *Separation and purification technology*, *192*, 441-456.
- Hanley, P. J., Mei, Z., Durett, A. G., da Graca Cabreira-Harrison, M., Klis, M., Li, W., . . . Mir, O. (2014). Efficient manufacturing of therapeutic mesenchymal stromal cells with the use of the Quantum Cell Expansion System. *Cytotherapy*, *16*(8), 1048-1058.
- Karst, D. J., Steinebach, F., & Morbidelli, M. (2018). Continuous integrated manufacturing of therapeutic proteins. *Current opinion in biotechnology*, *53*, 76-84.
- Kurosawa, H., Märkl, H., Niebuhr-Redder, C., & Matsumura, M. (1991). Dialysis bioreactor with radial-flow fixed bed for animal cell culture. *Journal of fermentation and bioengineering*, 72(1), 41-45.
- Lao, M. S., & Toth, D. (1997). Effects of ammonium and lactate on growth and metabolism of a recombinant Chinese hamster ovary cell culture. *Biotechnology progress*, 13(5), 688-691.
- Lu, R.-M., Hwang, Y.-C., Liu, I.-J., Lee, C.-C., Tsai, H.-Z., Li, H.-J., & Wu, H.-C. (2020). Development of therapeutic antibodies for the treatment of diseases. *Journal of biomedical science*, *27*(1), 1-30.
- Märkl, H., Zenneck, C., Dubach, A. C., & Ogbonna, J. C. (1993). Cultivation of Escherichia coli to high cell densities in a dialysis reactor. *Applied microbiology and biotechnology*, *39*(1), 48-52.
- Markvicheva, E., & Grandfils, C. (2004). Microcarriers for animal cell culture. In *Fundamentals of cell immobilisation biotechnology* (pp. 141-161): Springer.
- Martens, D., Nollen, E., Hardeveld, M., van der Velden-De Groot, C., De Gooijer, C., Beuvery, E., & Tramper, J. (1996). Death rate in a small air-lift loop reactor of vero cells grown on solid microcarriers and in macroporous microcarriers. *Cytotechnology*, *21*(1), 45-59.
- Merten, O.-W. (2015). Advances in cell culture: anchorage dependence. *Philosophical Transactions of the Royal Society B: Biological Sciences, 370*(1661), 20140040.
- Mizukami, A., de Abreu Neto, M. S., Moreira, F., Fernandes-Platzgummer, A., Huang, Y.-F., Milligan, W., . . . Swiech, K. (2018). A fully-closed and automated hollow fiber bioreactor for clinical-grade manufacturing of human mesenchymal stem/stromal cells. *Stem Cell Reviews and Reports,* 14(1), 141-143.
- Nakano, K., Rischke, M., Sato, S., & Märkl, H. (1997). Influence of acetic acid on the growth of Escherichia coli K12 during high-cell-density cultivation in a dialysis reactor. *Applied microbiology and biotechnology*, 48(5), 597-601.
- Nienow, A. W. (2006). Reactor engineering in large scale animal cell culture. Cytotechnology, 50(1-3), 9.
- Ozturk, S. S., Riley, M. R., & Palsson, B. O. (1992). Effects of ammonia and lactate on hybridoma growth, metabolism, and antibody production. *Biotechnology and bioengineering*, *39*(4), 418-431.
- Pakos, V., & Johansson, A. (1985). Large scale production of human fibroblast interferon in multitray battery systems. *Developments in biological standardization, 60,* 317.
- Pörtner, R., & Märkl, H. (1998). Dialysis cultures. *Applied microbiology and biotechnology, 50*(4), 403-414.
- Reuveny, S., Velez, D., Miller, L., & Macmillan, J. (1986). Comparison of cell propagation methods for their effect on monoclonal antibody yield in fermentors. *Journal of immunological methods,* 86(1), 61-69.

- Roberts, I., Baila, S., Rice, R. B., Janssens, M. E., Nguyen, K., Moens, N., . . . Mason, C. (2012). Scale-up of human embryonic stem cell culture using a hollow fibre bioreactor. *Biotechnology letters*, 34(12), 2307-2315.
- Rodriguez, J., Spearman, M., Tharmalingam, T., Sunley, K., Lodewyks, C., Huzel, N., & Butler, M. (2010). High productivity of human recombinant beta-interferon from a low-temperature perfusion culture. *Journal of biotechnology*, *150*(4), 509-518.
- Rowley, J., Abraham, E., Campbell, A., Brandwein, H., & Oh, S. (2012). Meeting lot-size challenges of manufacturing adherent cells for therapy. *Bioprocess Int*, 10(3), 7.
- Sheu, J., Beltzer, J., Fury, B., Wilczek, K., Tobin, S., Falconer, D., . . . Bauer, G. (2015). Large-scale production of lentiviral vector in a closed system hollow fiber bioreactor. *Molecular Therapy-Methods & Clinical Development, 2*, 15020.
- Tsao, Y.-S., Cardoso, A., Condon, R., Voloch, M., Lio, P., Lagos, J., . . . Liu, Z. (2005). Monitoring Chinese hamster ovary cell culture by the analysis of glucose and lactate metabolism. *Journal of biotechnology*, 118(3), 316-327.
- Valkama, A. J., Oruetxebarria, I., Lipponen, E. M., Leinonen, H. M., Käyhty, P., Hynynen, H., . . . Heikura, T. (2020). Development of large-scale downstream processing for lentiviral vectors. *Molecular Therapy-Methods & Clinical Development*, 17, 717-730.
- Walker, N. (2017). Perfusion Appears to be Gaining Traction in Biopharma Manufacturing. Retrieved from https://www.pharmoutsourcing.com/Featured-Articles/340000-Perfusion-Appears-to-be-Gaining-Traction-in-Biopharma-Manufacturing/
- Walsh, G. (2014). Biopharmaceutical benchmarks 2014. Nature Biotechnology, 32(10), 992-1000.
- Walsh, G. (2018). Biopharmaceutical benchmarks 2018. Nature biotechnology, 36(12), 1136-1145.
- Wang, S., Godfrey, S., Ravikrishnan, J., Lin, H., Vogel, J., & Coffman, J. (2017). Shear contributions to cell culture performance and product recovery in ATF and TFF perfusion systems. *Journal of biotechnology, 246*, 52-60.
- Wang, Z., Xue, J., Sun, H., Zhao, M., Wang, Y., Chu, J., & Zhuang, Y. (2020). Evaluation of mixing effect and shear stress of different impeller combinations on nemadectin fermentation. *Process Biochemistry*.
- Whaley, K. J., & Zeitlin, L. (2021). Emerging antibody-based products for infectious diseases: Planning for metric ton manufacturing. *Human Vaccines & Immunotherapeutics*, 1-11.
- Woodside, S. M., Bowen, B. D., & Piret, J. M. (1998). Mammalian cell retention devices for stirred perfusion bioreactors. *Cytotechnology*, *28*(1-3), 163-175.
- Xu, S., & Chen, H. (2016). High-density mammalian cell cultures in stirred-tank bioreactor without external pH control. *Journal of biotechnology*, 231, 149-159.
- YekrangSafakar, A., Hamel, K. M., Mehrnezhad, A., Jung, J. P., & Park, K. (2020). Development of rolled scaffold for high-density adherent cell culture. *Biomedical Microdevices*, 22(1), 4.
- Zhang, Y., Stobbe, P., Silvander, C. O., & Chotteau, V. (2015). Very high cell density perfusion of CHO cells anchored in a non-woven matrix-based bioreactor. *Journal of biotechnology*, *213*, 28-41.

Figure legends

Figure 1 Schematic diagram of rolled scaffold (RS) and RS bioreactor. (a) RS is made by rolling multiple layers to create a uniform gap between them. (b) RS is placed in a holder and the culture medium flows through its gap. Cells are growing on the internal surfaces of RS. (c) Simplified schematics of a RS bioreactor. The sensors at upstream and downstream can provide real-time assessment of combined cellular metabolism.

Figure 2 Structures of Mesh-RS and Fiber-RS. (a) Different layer structures of UV-RS, Mesh-RS, and Fiber-RS with their cross-section image. (b) The surface area increases quadratically by increasing the radius of the RS. L is the length of RS. (c) A phase-contrast image and (d) a fluorescent confocal image of CHO cells growing on the fiber layer.

Figure 3 Expansion of CHO-K1 cells in Mesh-RS. (a) Dissolved oxygen concentrations at upstream and downstream were measured during the culture period. The flow rate was increased to provide more oxygen to cells. (b) The oxygen consumption increased exponentially over time. Number of harvested cells at the end of each expansion is shown in boxes. (c) The number of cells inside the RS has a linear correlation to the amount of oxygen they consume. Comparing (d) the average growth rate and (e) the oxygen consumption rate of cells growing in medium and small Mesh-RSs shows little difference.

Figure 4 The growth of CHO-K1 cell in Fiber-RS. (a) The oxygen consumption increased exponentially, indicating an exponential growth for the initial 5 days. In Fiber-RS #1, cells were maintained for 10 days by changing the media on day 6 and reducing the temperature from 37°C to 34°C on day 7. (b) The cumulative consumption of glucose increased exponentially before cells

reached saturation on day 7. (c) The cell-specific glucose consumption rate in Fiber-RSs over different cell densities.

Figure 5 RS bioreactor with dialysis module. (a) Configuration of a RS dialysis bioreactor. Peristatic pumps are not shown. (b) CHO-K1 cells can be cultured for more than 10 days without replacing the media. During this period, air pressure in the flask was adjusted and supplements were added to provide adequate oxygen and nutrient to the cells. (c) After performing the dialysis on day 5, 92% of the lactate in media flask was removed and the glucose concentration was fully recovered. (d) The total amounts of glucose and lactate were preserved during the dialysis.

Figure 6 Comparing the growth rate of CHO cells in different high cell density bioreactors. Cells in RS bioreactors consistently showed a higher growth rate even at high cell densities until the cell population saturated.

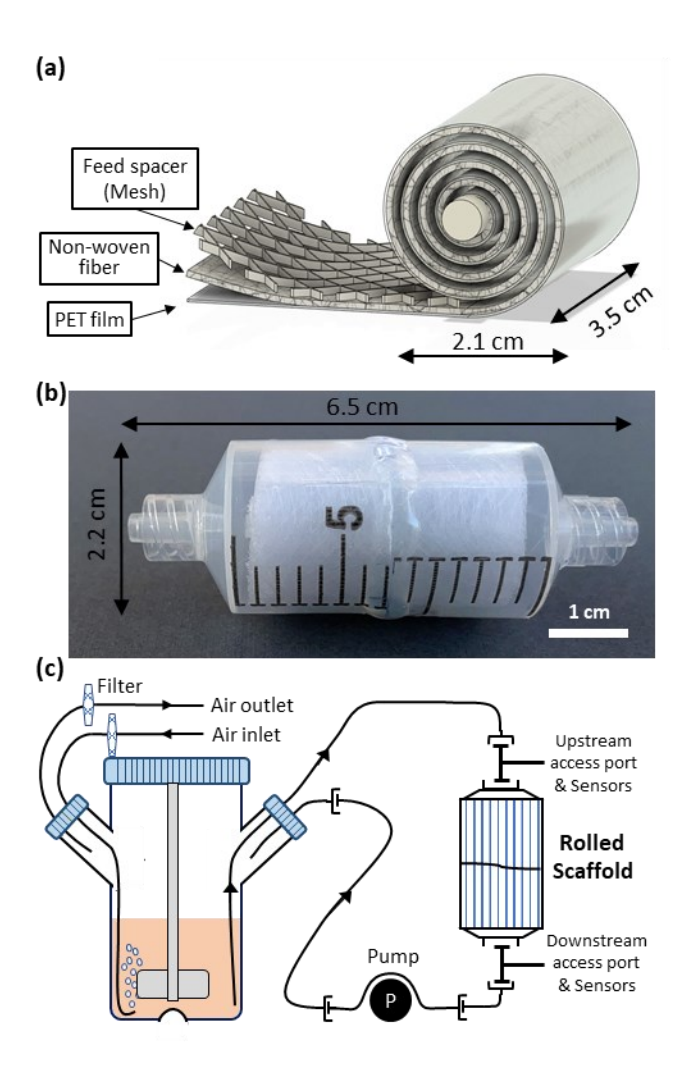


Figure 1 Schematic diagram of rolled scaffold (RS) and RS bioreactor. (a) RS is made by rolling multiple layers to create a uniform gap between them. The dimensions are based on medium-size RS which can provide 1700 cm² of culture surface. (b) RS is placed in a holder and the culture medium flows through its gap. Cells are growing on the internal surfaces of RS. (c) Simplified schematics of a RS bioreactor. The sensors at upstream and downstream can provide real-time assessment of combined cellular metabolism.

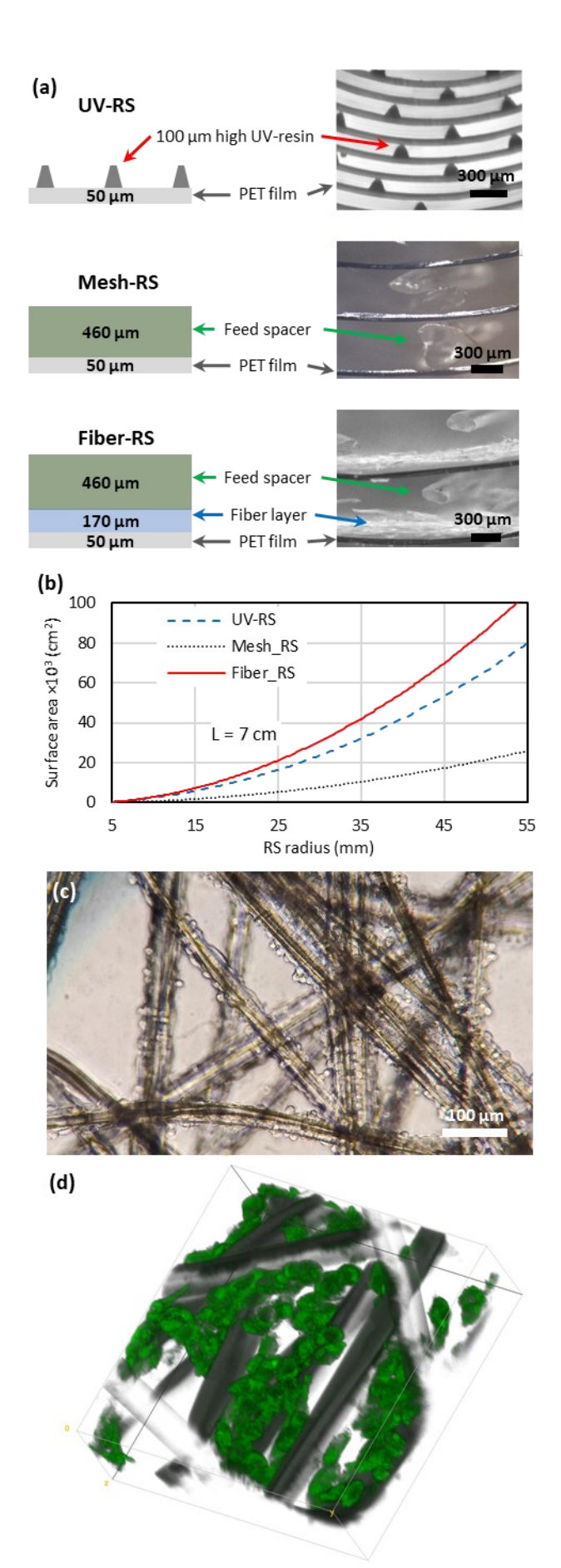


Figure 2 Structures of Mesh-RS and Fiber-RS. (a) Different layer structures of UV-RS, Mesh-RS, and Fiber-RS with their cross-section image. (b) The surface area increases quadratically by increasing the radius of the RS. L is the length of RS. (c) A phase-contrast image and (d) a fluorescent confocal image of CHO cells growing on the fiber layer.

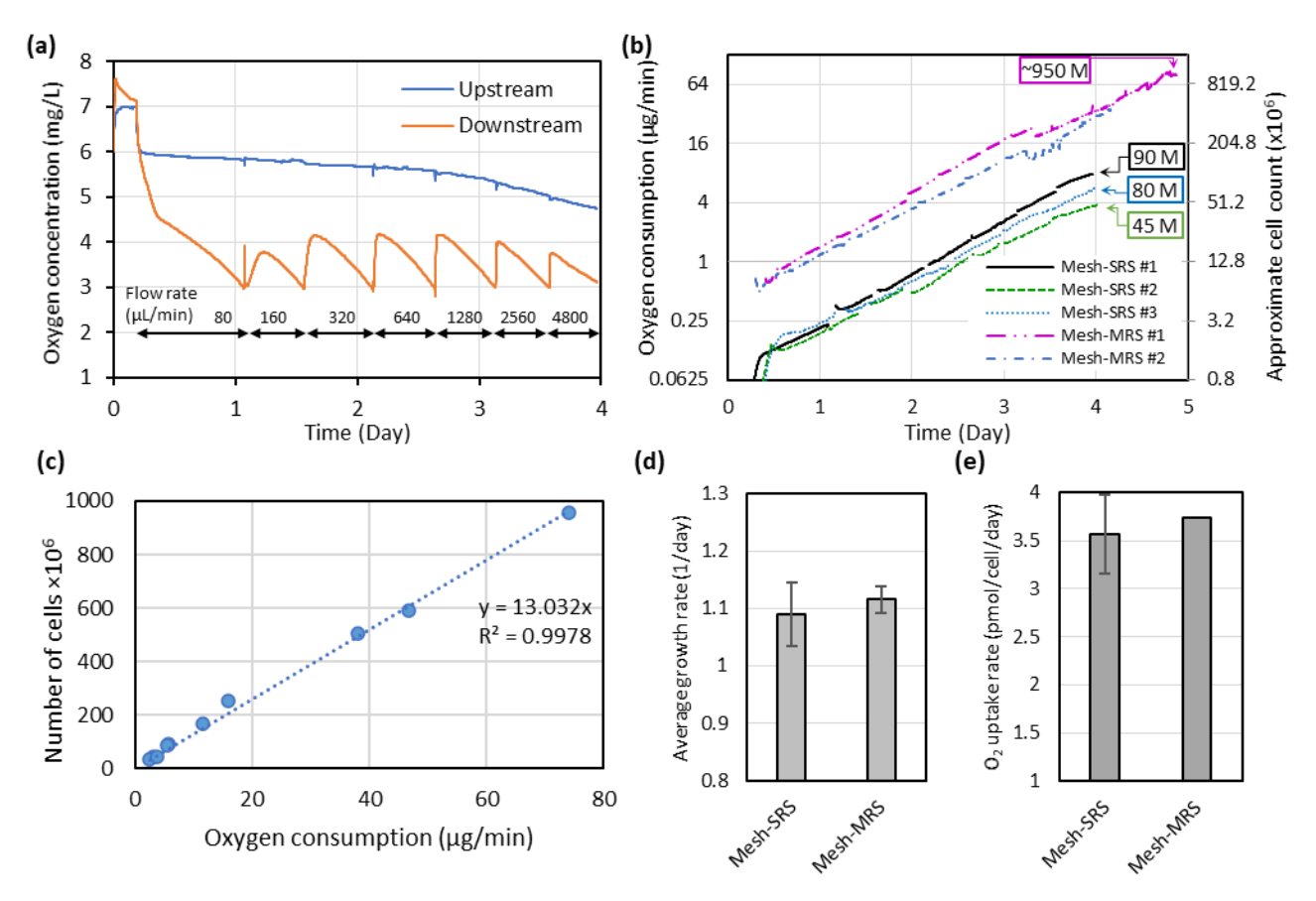


Figure 3 Expansion of CHO-K1 cells in Mesh-RS. (a) Dissolved oxygen concentrations at upstream and downstream were measured during the culture period. The flow rate was increased to provide more oxygen to cells. (b) The oxygen consumption increased exponentially over time. Number of harvested cells at the end of expansion is shown in boxes. (c) The number of cells inside the RS has a linear correlation to the amount of oxygen they consume. Comparing (d) the average growth rate and (e) the oxygen consumption rate of cells growing in medium and small Mesh-RSs shows little difference.

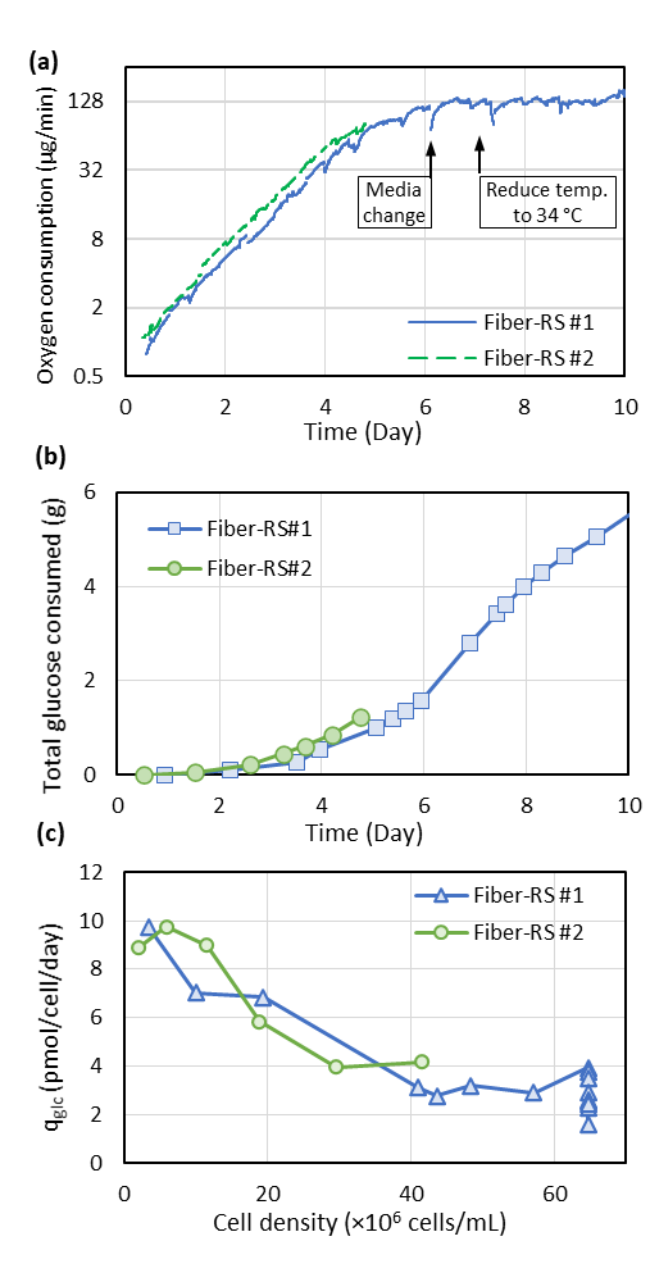


Figure 4 The growth of CHO-K1 cell in Fiber-RS. (a) The oxygen consumption increased exponentially, indicating an exponential growth for the initial 5 days. In Fiber-RS #1, cells were maintained for 10 days by changing the media on day 6 and reducing the temperature from 37°C to 34°C on day 7. (b) The cumulative consumption of glucose increased exponentially before cells reached saturation on day 7. (c) The cell-specific glucose consumption rate in Fiber-RSs over different cell densities.

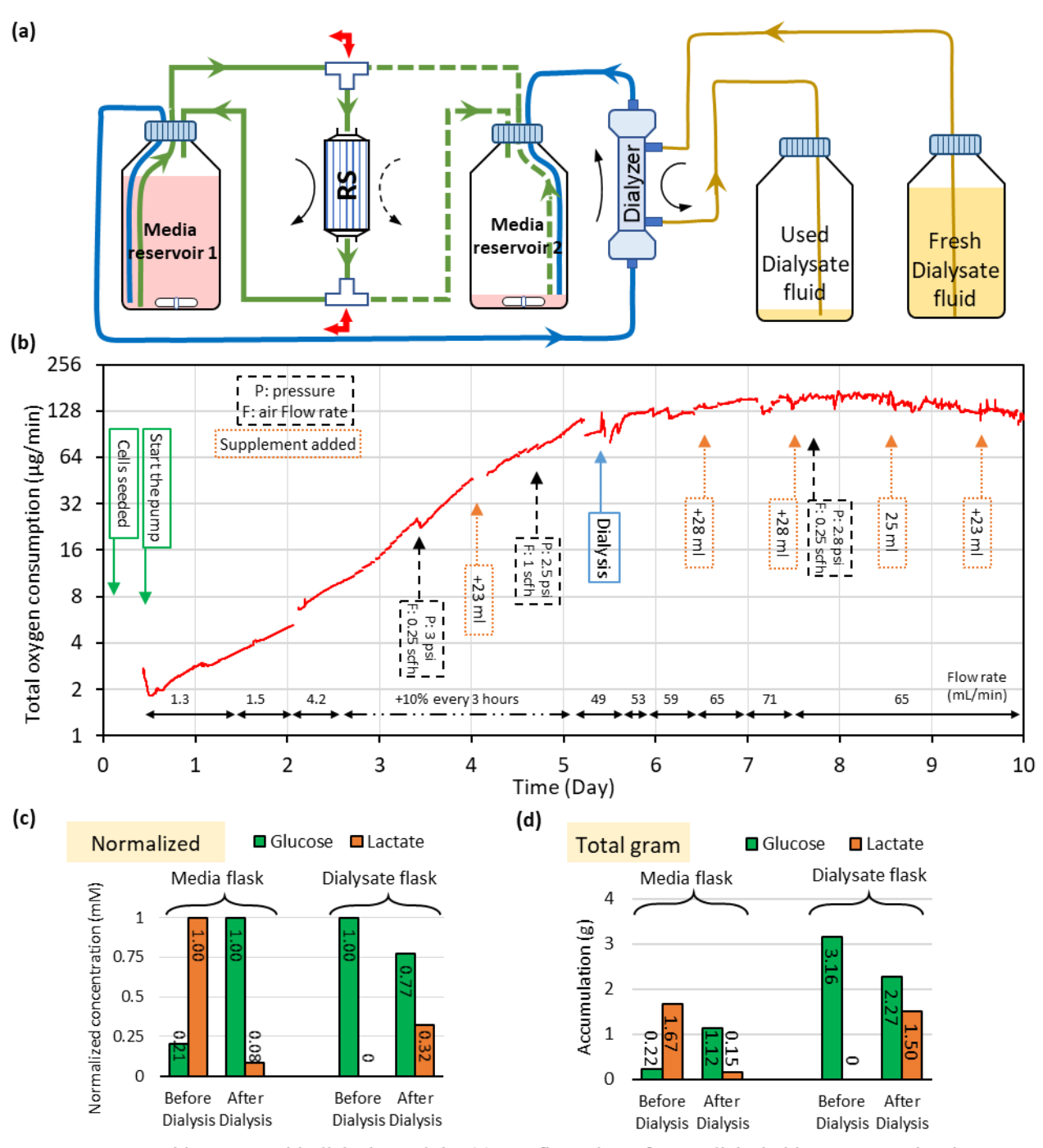


Figure 5 RS bioreactor with dialysis module. (a) Configuration of a RS dialysis bioreactor. Peristatic pumps are not shown. (b) CHO-K1 cells can be cultured for more than 10 days without replacing the media. During this period, air pressure in the flask was adjusted and supplements were added to provide adequate oxygen and nutrient to the cells. (c) After performing the dialysis on day 5, 92% of the lactate in media flask was removed and the glucose concentration was fully recovered. (d) The total amounts of glucose and lactate were preserved during the dialysis.

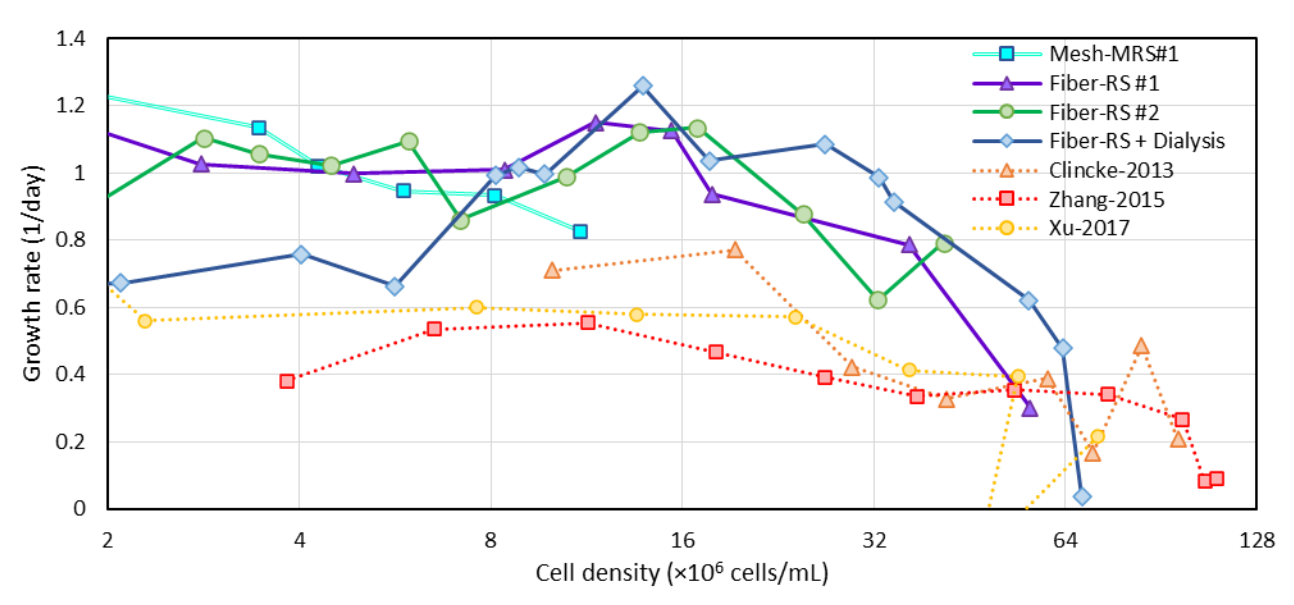
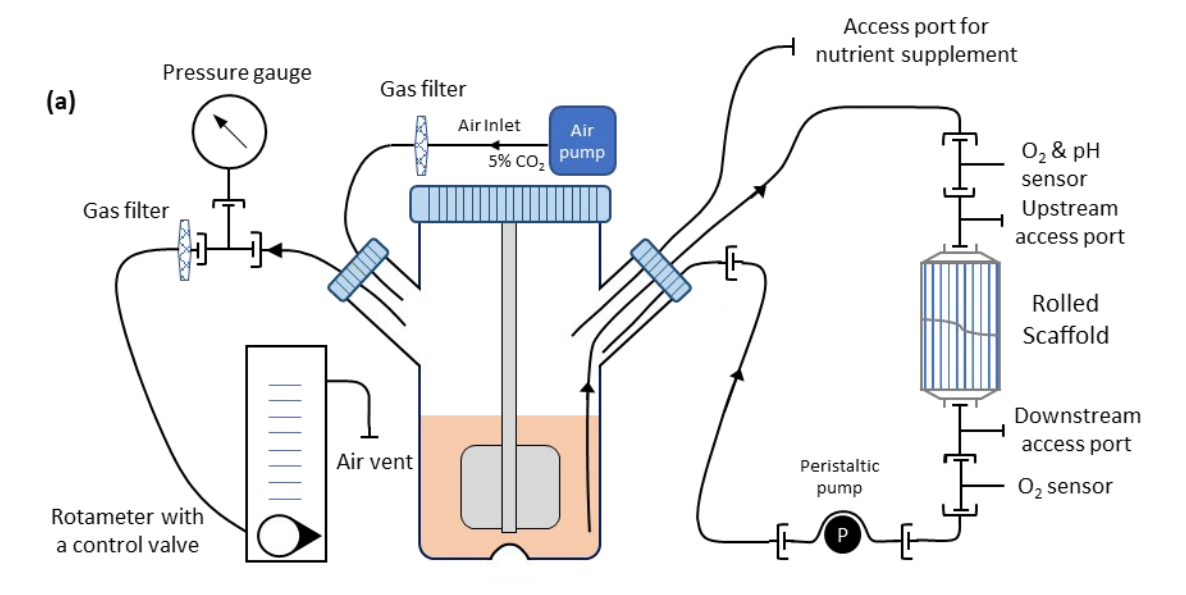


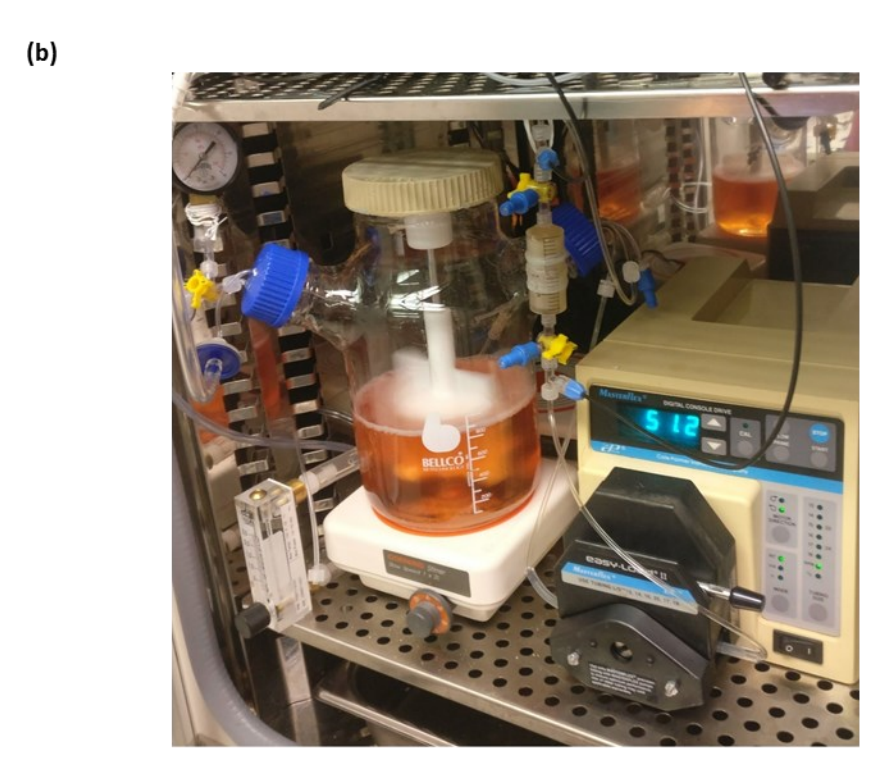
Figure 6 Comparing the growth rate of CHO cells in different high cell density bioreactors. Cells in RS bioreactors consistently showed higher growth rate even at high cell densities until the cell population saturated.

Supplementary Table S1. Dimension and key numbers of each RS variants.

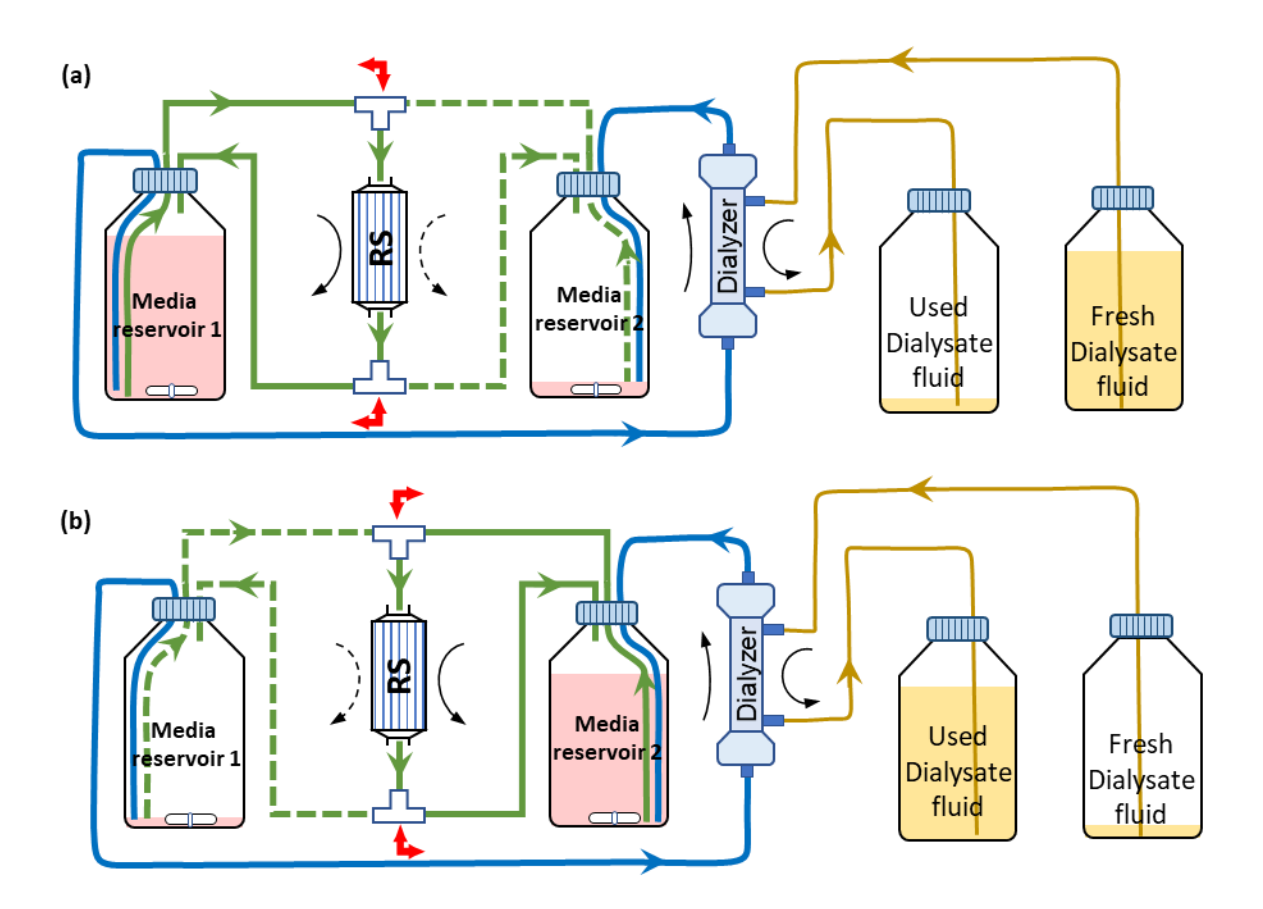
Type	UV_RS		Mesh_RS		Fiber_RS	
(height of channels)	(h = 100 μm)		(h = 460 μm)		(h = 630 μm)	
RS Size	Small	Medium	Small	Medium	Medium (No Dialysis)	Medium (W/ Dialysis)
Max. Cell number achieved	45 M	958 M	90 M	700 M	1712 M	2010 M
RS Volume ¹	2.73 mL	15.6 mL	17.7 mL	55 mL	25.4 mL	27.6 ml
Max. cell density achieved	16.4 M	60.8 M	5.1 M	12.8 M	67.4 M	72.3 M
	cells/mL	cells/mL	cells/mL	cells/mL	cells/mL	cells/mL
RS dimension	4.5 mm ×	10.8 mm ×	7.5 mm ×	10.8 mm ×	10.8 mm ×	11.2 mm ×
(radius × height)	43 mm	43 mm	100 mm	150 mm	70 mm	70 mm
Surface area	251 cm ²	1831 cm ²	520 cm ²	1950 cm ²	3272 cm ²	3800 cm ²
Surface area /	91.7	117.3	29.4	35.8	128.8	136.7
RS Volume	cm²/mL	cm²/mL	cm²/mL	cm²/mL	cm²/mL	cm²/mL
Effective cell suspension volume in RS (seeding) ²	1.2 mL	9.1 mL	9 mL	45 mL	23 mL	25 mL
Total used cell suspension volume (seeding) ³	3 ml @	16 ml @	18 ml @	55 ml @	30 ml @	30 ml @
	1 M cells/mL	1 M cells/mL	200K cells/mL	200K cells/mL	800K cells/mL	800K cells/mL

- 1) RS volume: Volume of the RS based on its external dimension.
- **2) Effective cell suspension volume in RS:** The volume that is needed to fill up the inner space of the RS. The number of the seeded cells is the product of the cell suspension concentration and this volume.
- **3) Total used cell suspension volume:** The volume of cells suspension that was injected to the RS holder. We injected more volume to account for the dead space in the RS holder.





Supplementary Figure S1. (a) Detailed configuration of a RS bioreactor. (b) The RS bioreactor in a $\rm CO_2$ incubator.



Supplementary Figure S2. Detailed configuration of a RS bioreactor with dialysis module (a) at the start of dialysis and (b) at the end of dialysis process.